Energy Harvesting from Jamming Attacks in Multi-User Massive MIMO Networks

Hayder Al-Hraishawi, *Member, IEEE*, Osamah A. Abdullah, *Member, IEEE*,
Symeon Chatzinotas, *Senior Member, IEEE,* and Björn Ottersten, *Fellow, IEEE*

***Abstract*—5G communication systems enable new functions and major performance improvements but at the cost of tougher energy requirements on mobile devices. One of the effective ways to address this issue along with alleviating the environmental effects associated with the inevitable large increase in energy usage is the energy-neutral systems, which operate with the energy harvested from radio-frequency (RF) transmissions. In this direction, this paper investigates the notion of harvesting the ambient RF signals from an unusual source. Specifically, the performance of an RF energy harvesting scheme for multi-user massive multiple-input multiple-output (MIMO) is investigated in the presence of multiple active jammers. The key idea is to exploit the jamming transmissions as an energy source to be harvested at the legitimate users. To this end, the achievable uplink sum rate expressions are derived in closed-form for two different antenna configurations. Two optimal time-switching schemes are also proposed based on maximum sum rate and user-fairness criteria. Besides, the essential trade-off between the harvested energy and achievable sum rate are quantified in closed-form. Our analysis reveals that the massive MIMO systems can exploit the surrounding RF signals of the jamming attacks for boosting the amount of harvested energy at the served users. Finally, numerical results illustrate the effectiveness of the derived closed-form expressions through simulations.**

I. Introduction

User devices in beyond 5G systems will essentially be empowered by artificial intelligence (AI) processing capabilities, which raises the energy requirements and makes users more power hungry due to the high computational loads [2]. Meanwhile, energy harvesting from ambient radio frequency (RF) signals has emerged as a sustainable solution for the tremendous growth in the energy consumption of wireless networks. Energy harvesting technologies can facilitate establishing energy efficient networks in order to not only cut down operational expenditures but also to address the growing concerns about the global environmental consequences due to operating the communication infrastructures using fossil fuel. Moreover, since future wireless networks will be more densified and the communication distances are becoming much shorter, wireless energy harvesting will be more meaningful and feasible for the users within the applications that have limited power supplies [3]. However, there are some practical limitations inhibit harvesting enough energy at the receivers such as the low RF energy to direct current (DC) conversion efficiency and the severe pathloss between the transmitter and the receiver. Towards this end, smart antennas technologies such as massive MIMO that can enhance the performance of energy harvesting and then boost the overall energy efficiency and achievable data rate [4].

The concept of energy harvesting has been widely adopted in massive MIMO systems, where some of the prior related works can be outlined as follows. In [5], an energy harvesting strategy has developed and analyzed to power the secondary users of a cognitive radio system through harvesting energy from primary user transmissions. Reference [6] has proposed and analyzed an architecture of self-backhaul and energy harvesting small cell network with massive MIMO. In [7], the trade-off between the achievable rate and harvested energy has been analyzed at massive MIMO receivers, where a low-complexity antenna partitioning algorithm for energy harvesting massive MIMO systems is proposed. Authors in [8] have investigated the feasibility of utilizing a relay-assisted massive MIMO to enhance the performance of simultaneous wireless information and power transfer (SWIPT) by leveraging the excess degrees-of-freedom offered by massive antenna arrays at the base-station. Further, optimizing the downlink transmission for simultaneous wireless information and power transfer (SWIPT) in multi-cell massive MIMO systems is analyzed in [9] with the existence of a two-antenna energy harvester that is capable of harvesting energy via one antenna, and eavesdropping upon the legitimate communications via the other antenna.

Furthermore, massive MIMO as a concept is developed to accommodate the massive connectivity requirement that is essential for future wireless cellular networks to support machine-type communications (MTC) and Internet of things (IoT) devices [10], [11]. Nevertheless, ubiquitous wireless connectivity is appealing to the envisioned beneficiaries of these networks as well as to the bad actors where they can wreak havoc by actively eavesdropping and/or jamming. Moreover, jamming devices used to be implemented on high-cost hardware mostly for military purposes but currently they can be realized through modifying the firmware of commodity hardware [12]. Additionally, active jammers need a sufficiently high energy budget for each transmission block, which is allocated between pilot spoofing attacks during channel training phase and jamming the legitimate communications

H. Al-Hraishawi, S. Chatzinotas, and B. Ottersten are with the Interdisciplinary Centre for Security, Reliability and Trust (SnT), University of Luxembourg, L-1855, Luxembourg.

O. A. Abdullah is with the Department of Electrical Engineering, Alma'moon University College, Baghdad, Iraq.

Corresponding author: *Hayder Al-Hraishawi (hayder.al-hraishawi@uni.lu)*.

This work in part was presented at IEEE International Conference on Communications (ICC), 2021 [1]. For the purpose of open access, the authors have applied a Creative Commons Attribution 4.0 International (CC BY 4.0) license to any Author Accepted Manuscript version arising from this submission.

during data transmission phase [13]. Interestingly, this high-power jamming signals can be exploited at the legitimate user devices. Specifically, different from the existing research works in the context of RF energy harvesting, this paper intends to investigate using the jamming energy transmitted by the jammers to be harvested at the users.

In the context of detecting the jamming threats, there have been abundant contributions in the literature that have proposed many effective approaches to deal with these security challenges. In particular, a detailed survey article on the methods and techniques that are employed for detecting active attacks on massive MIMO systems can be found in [14] . On the other hand, jamming defense strategies for massive MIMO are developed in [15] in which secret keys are employed to encrypt and protect the legitimate communications from the jamming attacks. Likewise, a full-stack framework for detecting and suppressing jamming attacks in cell-free massive MIMO system is proposed in [16] to utilize the unused pilots for designing a jammer detector based on the likelihood functions of the measured signals. Moreover, based on game theory, a beam-domain jamming defense approach is developed in [17] for suppressing the malicious attacks on the downlink transmissions of the massive MIMO systems. In [18], a jamming-resistant receiver scheme has been proposed to utilize the high spatial resolution of massive MIMO for enhancing the robustness of uplink transmissions.

The multi-antenna massive MIMO base-station can be used for provisioning physical layer security by exploiting the large antenna arrays to simultaneously transmit confidential signals towards the legitimate user nodes and artificial noise (AN) sequences towards eavesdroppers for perturbing their intercepted signals, and hence, improving the secrecy performance [19]. In this direction, the communication secrecy aspects of massive MIMO systems in the presence of active and passive attacks have been extensively studied in multiple works [18]–[24]. Specifically, securing the millimeter-wave (mm-Wave) massive MIMO channels by exploiting the spatial sparsity of legitimate user's channel has been studied in [24]. The proposed security scheme in [24] is based on processing information data onto dominant angle components of the sparse channel, while AN is broadcast over the remaining non-dominant angles interfering only with the eavesdropper with a higher probability. Nevertheless, we will not delve into similar mechanisms that pursue strengthening the communication security or incapacitating the eavesdropper's ability to decode the confidential data, which are beyond the scope of this work. Instead, we focus on exploiting the jamming transmissions of the active attackers as a viable source for energy harvesting, and thus, increasing the energy efficiency of massive MIMO networks. Specifically, the objective of this paper is to make full use of the RF energy in wireless environment.

The design of an energy-harvesting receiver under jamming attacks has been investigated in some prior works based on the premise that the detrimental interference can be harvested to increase the transmit power [25]–[27]. Specifically, an energy-harvesting receiver for two-way orthogonal frequency division multiplexing (OFDM) systems under hostile jamming is designed to simultaneously process information and harvest energy from the received desired signals as well as the jamming interference through a power splitter [25]. In [26], the authors show that energy harvesting can be exploited for counteracting the jamming interference in a wireless secret key generation (SKG) system that consists of a pair of legitimate nodes and a malicious jammer. In the same context, a strategic interaction framework between a pair of legitimate user nodes and a jammer have been formulated as a zero-sum game in [27], and the analysis has demonstrated that the legitimate user are capable of neutralizing the jammer by appropriately tuning the transmit power and the energy harvesting duration. Nevertheless, to the best of our knowledge, this concept has not been studied yet in the open literature on a whole system level by considering multiple legitimate users attacked by multiple jammers. Therefore, this observation motivates this work to study the performance of a massive MIMO system utilizes the jamming attacks to power the legitimate users.

The key technical contributions of this study can be summarized as follows:

- Developing a novel RF energy harvesting scheme for massive MIMO to fully utilize the ambient RF signals. Specifically, the legitimate user nodes can harvest energy from the jamming transmissions of the active attackers in order to utilize this energy for sending their payload data to the base-stations.
- Formulating and deriving the essential performance metrics of the proposed energy-harvesting scheme for finite/infinite antenna regime at the base-station with taking into account the accumulative impact of the imperfect channel state information (CSI) and co-channel interference. We consider the uplink transmissions in order to evaluate the achievable data rate by the users when the proposed energy harvesting scheme is employed.
- Designing two optimal time-switching energy harvesting control schemes for the users based on the sum rate maximization and max-min user-fairness criteria.
- Analyzing the energy-rate trade-off in the time-switching energy harvesting protocol, and deriving this interaction in a closed-form expression. Numerical/simulation results are presented to validate our analysis and to obtain system-design insights.

The rest of the paper is structured as follows. The considered system model is presented in Section II. The performance metrics for both limited and unlimited antenna arrays at the base-station alongside with optimization of time-switching factor and the energy-rate trade-off analysis are all derived and presented in Section III. Numerical results and discussions on our proposed scheme are provided in Section IV. Finally, Section V summarizes the concluding remarks.

Notation: $\mathbf{Z}^H$ and $[\mathbf{Z}]_{i,j}$ denote the Hermitian-transpose and the $(i,j)\text{th}$ element of the matrix $\mathbf{Z}$, respectively. The absolute value and norm operator are denoted by $|\cdot|$ and $\|\cdot\|$, respectively. $\mathbb{E}[z]$ and $\mathbb{V}\text{ar}[z]$ are the expected value and the variance of z, and the operator $\otimes$ denotes the Kronecker product. $\text{Ei}(z)$ is the exponential integral function for the positive values of the real part of z. Finally, the notation $\mathbf{Z} \sim \mathcal{CN}(\mathbf{0}, \mathbf{\Sigma})$ denotes that $\mathbf{Z}$ is a circularly symmetric complex Gaussian distributed

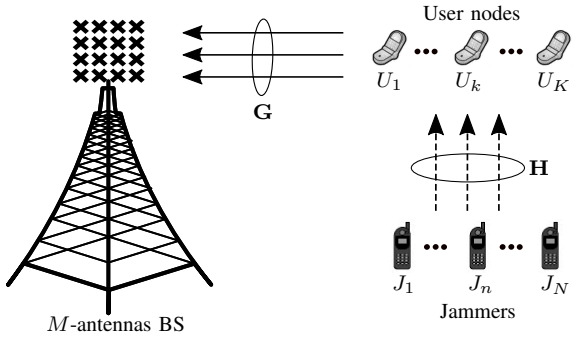

Fig. 1. Multi-user massive MIMO uplink transmissions under attacks by multiple jammers.

with zero mean and covariance matrix $\mathbf{\Sigma}$.

II. System, channel, and signal models

In this section, the system, channel, and signal models are presented in details along with analyzing the energy harvesting model in massive MIMO networks.

A. System and channel models

We consider the uplink transmission of a multi-user massive MIMO network that consists of an M-antennas base-station to serve K randomly distributed user nodes (U_k) for $k \in \{1, \cdots, K\}$ in the presence of N randomly located active jammers (J_n) for $n \in \{1, \cdots, N\}$. Each user node and jammer is herein assumed to be equipped with a single antenna as shown in Fig. 1. This model captures the key idea of jamming multiple concurrent communications and our analysis can be readily generalized to the case of multi-cell systems.

Let $\mathbf{G} \in \mathbb{C}^{(M \times K)}$ be the channel matrix between the base-station and user nodes, which can be modeled as

$$\mathbf{G} = \tilde{\mathbf{G}} \mathbf{D}_G^{1/2}, \tag{1}$$

where $\tilde{\mathbf{G}} \sim \mathcal{CN}_{M \times K}(\mathbf{0}_{M \times K}, \mathbf{I}_M \otimes \mathbf{I}_K)$ accounts for the independent small-scale Rayleigh fading, and diagonal matrix $\mathbf{D}_G = \text{diag}(\zeta_{G_1}, \cdots, \zeta_{G_k}, \cdots, \zeta_{G_K})$ captures the large-scale fading including path-loss and shadowing.

User nodes can harvest energy from the jamming transmissions of the active eavesdroppers through the jamming channel $\mathbf{H}$, which can be defined as

$$\mathbf{H} = \tilde{\mathbf{H}} \mathbf{D}_H^{1/2}, \tag{2}$$

where $\tilde{\mathbf{H}} \sim \mathcal{CN}_{K \times N}(\mathbf{0}_{K \times N}, \mathbf{I}_K \otimes \mathbf{I}_N)$ captures the independent small-scale Rayleigh fading channel, and $\mathbf{D}_H$ accounts the energy harvesting channel large-scale fading. Here, the elements of $\mathbf{D}_H$ can be vectorized as $\text{vec}[\mathbf{D}_H] = [\beta_{H_{11}}, \cdots, \beta_{H_{1N}}, \cdots, \beta_{H_{KN}}]$.

A block-fading model has been considered in this analysis, where the channel remains constant during a coherence block of T_C symbol times, which is practically computed as the product of the coherence time and the coherence bandwidth. Signals consisting of T_C symbols can be transmitted in a coherence block and these signals can be represented by vectors of T_C lengths. Specifically, the considered massive MIMO system is operating in time-division duplex (TDD) mode, and the uplink transmission coherence block (T_C) of each user node is divided into three orthogonal time-slots as represented in Fig. 2. At the beginning of each coherence block, all user nodes simultaneously transmit orthogonal pilot sequences during (T_p) to the base-station for estimating their respective channels. Afterwards, user nodes harvest energy during αT, where $\alpha \in (0, 1)$ is the time-switching factor and $T = T_C - T_p$. The user nodes utilize the harvested energy for data transmission during the remaining time duration $(1-\alpha)T$. Meanwhile, we assume that the active jammers are constantly transmitting to jam the user nodes.

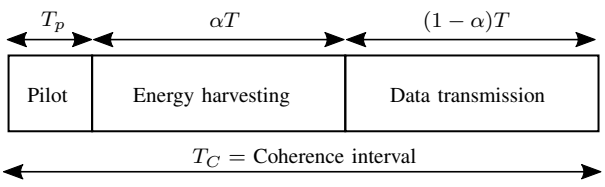

Fig. 2. A representation of a transmission frame in time-switching energy harvesting protocol for users, where $T = T_C - T_p$.

B. Acquisition of channel state information

In practice, the channels are estimated during the uplink channel training phase (T_p) at the base-station through uplink pilot sequences transmitted by the user nodes. Then, these uplink channel estimates are used by the base-station to obtain the downlink channels via channel reciprocity that holds in TDD systems [28], [29]. Specifically, at the beginning of the channel training phase, all user nodes transmit their pilot sequences $\mathbf{\Phi}_k \in \mathbb{C}^{(1 \times T_p)}$, where T_p is the pilot sequence length, satisfying $T_p \geq K$. Furthermore, $\mathbf{\Phi}_k \mathbf{\Phi}_k^H = 1$ and $\mathbf{\Phi}_k \mathbf{\Phi}_{k'}^H = 0$ when $k \neq k'$ and $k, k' \in \{1, \ldots, K\}$. Accordingly, the pilot signal received at the base-station can be written as

$$\mathbf{Y}_{\text{p}} = \sum_{k=1}^{K} \sqrt{T_p \mathcal{P}_p}\, \mathbf{g}_k \mathbf{\Phi}_k + \mathbf{N}_{\text{p}}, \tag{3}$$

where $\mathcal{P}_p$ is the average pilot transmit power of the user nodes, while $\mathbf{N}_{\text{p}}$ is an additive white Gaussian noise (AWGN) matrix whose elements are independent and identically distributed (i.i.d.) $\mathcal{CN}(0, 1)$ random variables. After projecting $\mathbf{Y}_{\text{p}}$ onto $\mathbf{\Phi}_k$, the minimum mean square error (MMSE) estimates of $\mathbf{g}_k$ can be derived as [30]

$$\hat{\mathbf{g}}_k = \sqrt{T_p \mathcal{P}_p} \zeta_{G_k} (1 + T_p \mathcal{P}_p \zeta_{G_k})^{-1}\, \mathbf{Y}_{\text{p}} \mathbf{\Phi}_k \tag{4}$$

The MMSE estimate of $\hat{\mathbf{G}}$ can be then written as $\hat{\mathbf{G}} = [\hat{\mathbf{g}}_1; \cdots; \hat{\mathbf{g}}_k; \cdots; \hat{\mathbf{g}}_K]$. The true channel of $\mathbf{G}$ can be written in terms of its estimate as

$$\mathbf{G} = \hat{\mathbf{G}} + \boldsymbol{\mathcal{E}}_G \tag{5}$$

where $\boldsymbol{\mathcal{E}}_G$ is the channel estimation error matrix. From the orthogonality property of MMSE, $\hat{\mathbf{G}}$ and $\boldsymbol{\mathcal{E}}_G$ are statistically independent and distributed as $\hat{\mathbf{G}} \sim \mathcal{CN}(0, \hat{\mathbf{D}}_G)$ and $\boldsymbol{\mathcal{E}}_G \sim \mathcal{CN}(0, \mathbf{D}_G - \hat{\mathbf{D}}_G)$, respectively, where $\hat{\mathbf{D}}_G$ is a diagonal matrix with the k-th diagonal element is given by $\hat{\zeta}_{G_k} = T_p \mathcal{P}_p \zeta_{G_k}^2 (1 + T_p \mathcal{P}_p \zeta_{G_k})^{-1}$.

C. Energy harvesting

Before deriving the achievable rate in the next Section III, we first obtain the harvested energy. During the second portion of uplink time-slot having a length of αT, user nodes harvest energy from the jamming transmissions. Thus, the average harvested energy at the k-th user can be computed as

$$E_{h_k} = \alpha T \, \Psi_{EH_k}(P_{I_k}), \tag{6}$$

where P_{I_k} is the incident power at the rectenna of the k-th user and can be defined by as

$$P_{I_k} = \left\| \mathbf{h}_k \mathbf{P}_E^{1/2} \right\|^2, \tag{7}$$

where $\mathbf{P}_E = \text{diag}(P_{E_1}, \cdots, P_{E_n}, \cdots, P_{E_N})$ accounts for the jamming powers of the active attackers for $n \in \{1, \cdots, N\}$, $\mathbf{h}_k$ is the k-th row of $\mathbf{H}$.

Moreover, in (6), $\Psi_{EH_k}(\cdot)$ is a non-linear function of the incident power P_{I_k}. The practical non-linear energy harvesting model in [31] is considered in this analysis because practically the harvested energy is a non-linear function of the incident RF power at the rectenna. Typically, the RF-to-direct current (RF-to-DC) energy conversion efficiency increases with the incident power until a peak, and then it saturates to a constant defined by the characteristics of energy harvesting circuitry. This non-linear model contradicts the linear energy harvesting model that has been considered in multiple studies as it largely overestimates the harvested energy in high incident power regime. The practically-viable non-linear operating characteristics of the energy harvesting circuitry is given in the following expression

$$\Psi(\rho) = \left[\frac{\delta}{1 - v} \left(\frac{1}{1 + e^{-\psi(\rho - w)}} - v \right) \right]^+, \tag{8}$$

where $[\lambda]^+ = \max(0, \lambda)$, $v = 1/(1+e^{\psi w})$, and ρ is the incident power. The parameters δ, ψ, and w capture various non-linear effects of energy harvesting circuitry, and they can be defined for practical energy harvesters as $\delta = 9.079\mu$W, $\omega = 2.9\mu$W.

User nodes utilize the harvested energy in (6) for transmitting their data to the base-station during the remaining time duration $(1-\alpha)T$, and thus, the uplink transmission power of the k-th user node can be defined as

$$P_{d_k} = \frac{E_{h_k}}{(1 - \alpha)T}. \tag{9}$$

D. Signal model for uplink transmission

This subsection considers modeling and analyzing the signal model for the massive MIMO uplink transmission. In particular, the received signal at the base-station after applying the zero-forcing[1] (ZF) detector can be written as

$$\mathbf{y}_U = \hat{\mathbf{W}} \left(\sqrt{\mathbf{P}_d} \mathbf{G} \mathbf{x}_d + \mathbf{n}_U \right), \tag{10}$$

where $\hat{\mathbf{W}}$ is the ZF detector at the base-station and is defined as

$$\hat{\mathbf{W}} = (\hat{\mathbf{G}}^H \hat{\mathbf{G}})^{-1} \hat{\mathbf{G}}^H. \tag{11}$$

[1]ZF-type receiver filter performs better than matched-filter detector in terms of nulling the jamming signal [18] and inter-pair interference mitigation [29].

In (10), $\mathbf{P}_d = \text{diag}(P_{d_1}, \cdots, P_{d_k}, \cdots, P_{d_K})$ is an $K \times K$ diagonal matrix representing the uplink transmit power for the K user nodes that obtained from (9) for $k \in \{1, \cdots, K\}$. Further, $\mathbf{x}_d$ is the transmitted vectors of the user nodes that satisfying $\mathbb{E}[\mathbf{x}_d \mathbf{x}_d^H] = \mathbf{I}_K$, and $\mathbf{n}_U \sim \mathcal{CN}(0, 1)$ is the AWGN at the base-station satisfying that $\mathbb{E}[\mathbf{n}_U \mathbf{n}_U^H] = \mathbf{I}_{n_U} \sigma_n^2$.

III. Performance Analysis

In this section, the achievable uplink sum rates are derived for two different antenna configurations at the base-station. This section also presents the optimization of the time-switching energy harvesting protocol in terms of maximum sum rate and user-fairness along with quantifying the trade-off between the harvested energy and uplink achievable rate.

A. Uplink sum rate for finite number of base-station antennas

In order to capture the joint impact of detection uncertainty, interference, and filtered AWGN, the k-th user data stream received at the base-station is written by using (10) as

$$\tilde{y}_k = \sqrt{P_{d_k}} \mathbb{E}\left[\hat{\mathbf{w}}_k \mathbf{g}_k \right] x_{d_k} + \tilde{n}_{U_k}, \tag{12}$$

where the first term accounts for the desired signal, and the second term represents the effective noise capturing the collective impacts of interference arises from detection uncertainty with imperfect CSI, inter-user interference, and filtered AWGN, which is expressed as

$$\begin{aligned} \tilde{n}_{U_k} = & \sqrt{P_{d_k}} \left(\hat{\mathbf{w}}_k \mathbf{g}_k - \mathbb{E}\left[\hat{\mathbf{w}}_k \mathbf{g}_k \right] \right) x_{d_k} \\ & + \sum_{k=1, k' \neq k}^{K} \sqrt{P_{d_{k'}}} \hat{\mathbf{w}}_k \mathbf{g}_{k'} x_{d_{k'}} + \hat{\mathbf{w}}_k n_{U_k}. \end{aligned} \tag{13}$$

An achievable uplink sum rate expression, that can tightly bound the ergodic sum rate, is derived by invoking the worst-case Gaussian approximation technique as follows [29]

$$\mathcal{R}_U = \frac{(1 - \alpha)T}{T_C} \sum_{k=1}^{K} \log_2 \left(1 + \tilde{\gamma}_k \right), \tag{14}$$

where $\tilde{\gamma}_k$ is the effective signal-to-interference-plus-noise ratio (SINR) of the k-th user node and is obtained as follows

$$\tilde{\gamma}_k = \frac{P_{d_k} \left| \mathbb{E}\left[\hat{\mathbf{w}}_k \mathbf{g}_k \right] \right|^2}{\text{BU}_k + \sum\limits_{k'=1, k' \neq k}^{K} \text{UI}_{kk'} + \sigma_n \mathbb{E}\left[\left\| \hat{\mathbf{w}}_k \right\|^2 \right]}, \tag{15}$$

where BU_k and $\text{UI}_{kk'}$ are the beamforming gain uncertainty and the interference caused by other users, respectively, which can be defined as

$$\text{BU}_k = P_{d_k} \mathbb{V}\text{ar}\left[\hat{\mathbf{w}}_k \mathbf{g}_k \right], \tag{16a}$$

$$\text{UI}_{kk'} = P_{d_{k'}} \mathbb{E}\left[\left| \hat{\mathbf{w}}_k \mathbf{g}_{k'} \right|^2 \right]. \tag{16b}$$

Next, the achievable uplink sum rate at the base-station can be derived in closed-form as follows. To begin with, the term $\hat{\mathbf{w}}_k \mathbf{g}_k$ in (5) can be simplified as follows:

$$\hat{\mathbf{w}}_k \mathbf{g}_k = \hat{\mathbf{w}}_k (\hat{\mathbf{g}}_k + \mathcal{E}_{G_k}) = 1 + \hat{\mathbf{w}}_k \mathcal{E}_{G_k}, \tag{17}$$

$$\bar{\mathcal{R}}_U^{\infty} = \frac{(1-\alpha)}{\ln(2)} \sum_{k=1}^{K} \sum_{j=1}^{N} \left(\prod_{i=1, i\neq j}^{N} \frac{\beta_{H_j} P_{E_j}}{\beta_{H_j} P_{E_j} - \beta_{H_i} P_{E_i}} \right) \left[-\exp\left(\frac{1}{\eta \mathcal{A}_k \beta_{H_j} P_{E_j}} \right) \mathrm{Ei}\left(\frac{-1}{\eta \mathcal{A}_k \beta_{H_j} P_{E_j}} \right) \right] \tag{29}$$

where $\mathcal{E}_{G_k}$ is the k-th column of estimation error matrix $\boldsymbol{\mathcal{E}}_G$. Since $\hat{\mathbf{w}}_k$ and $\mathcal{E}_{G_k}$ are uncorrelated and $\mathcal{E}_{G_k}$ is a zero-mean random variable, then $\mathbb{E}\left[\hat{\mathbf{w}}_k \mathcal{E}_{G_k}\right] = 0$. Therefore,

$$\mathbb{E}\left[\hat{\mathbf{w}}_k \mathbf{g}_k\right] = 1 + \mathbb{E}\left[\hat{\mathbf{w}}_k \mathcal{E}_{G_k}\right] = 1. \tag{18}$$

Next, the term accounts for the beamforming gain uncertainty BU_k can be derived by using (17) and (18) as

$$\begin{aligned}
\mathbb{V}\mathrm{ar}(\hat{\mathbf{w}}_k \mathbf{g}_k) &= \mathbb{E}\left[|\hat{\mathbf{w}}_k \mathcal{E}_{G_k}|^2 \right] \\
&= (\zeta_{G_k} - \hat{\zeta}_{G_k}) \mathbb{E}\left[\|\hat{\mathbf{w}}_k\|^2 \right] \\
&= (\zeta_{G_k} - \hat{\zeta}_{G_k}) \mathbb{E}\left[\left(\hat{\mathbf{G}}^H \hat{\mathbf{G}} \right)^{-1} \right]_{k,k} \\
&= \frac{(\zeta_{G_k} - \hat{\zeta}_{G_k})}{\hat{\zeta}_{G_k} K} \mathbb{E}[\mathrm{Tr}(\mathbf{X}^{-1})] \\
&= \frac{(\zeta_{G_k} - \hat{\zeta}_{G_k})}{\hat{\zeta}_{G_k} (M-K)},
\end{aligned} \tag{19}$$

where $\mathbf{X}$ is a $K \times K$ central Wishart matrix with N_P degrees of freedom and covariance matrix $\mathbf{I}_K$, where $\mathbb{E}[\mathrm{Tr}(\mathbf{X}^{-1})] = K/(M-K)$ [32].

The next term of the inter-user interference $\mathrm{UI}_{kk'}$ can be computed from (17), $\hat{\mathbf{w}}_k \mathbf{g}_{k'} = \hat{\mathbf{w}}_k \mathcal{E}_{G_{k'}}$ for $k' \neq k$. Since $\hat{\mathbf{w}}_k$ and $\mathcal{E}_{G_{k'}}$ are uncorrelated, then it can be shown that

$$\begin{aligned}
\mathbb{E}\left[|\hat{\mathbf{w}}_k \mathbf{g}_{k'}|^2 \right] &= \left(\zeta_{G_{k'}} - \hat{\zeta}_{G_{k'}} \right) \mathbb{E}\left[\left(\hat{\mathbf{G}}^H \hat{\mathbf{G}} \right)^{-1} \right]_{k,k} \\
&= \frac{\zeta_{G_{k'}} - \hat{\zeta}_{G_{k'}}}{\hat{\zeta}_{G_k} (M-K)}.
\end{aligned} \tag{20}$$

Similarly, the noise term obtains as

$$\sigma_n^2 \mathbb{E}\left[\|\hat{\mathbf{w}}_k\|^2 \right] = \frac{\sigma_n^2}{\hat{\zeta}_{G_k} (M-K)}. \tag{21}$$

Then, by substituting (18), (19), (20), and (21) into (15), the achievable rate of the k-th at the base-station can be derived as given below:

$$\bar{\mathcal{R}}_U = \frac{(1-\alpha)T}{T_C} \sum_{k=1}^{K} \log_2 \left(1 + \frac{P_{d_k} (M-K) \hat{\zeta}_{G_k}}{\sum_{k'=1}^{K} P_{d_{k'}} (\zeta_{G_{k'}} - \hat{\zeta}_{G_{k'}}) + \sigma_n^2} \right) \tag{22}$$

B. Uplink sum rate for large number of antennas

The asymptotic properties of massive MIMO is utilized in this subsection to obtain a closed-form expression of the asymptotic uplink sum rate. Namely, the number of antennas at the base-station grows unbounded with respect to the number of served user nodes, i.e., the number of users (K) is kept at arbitrary finite value with respect to M. Having been inspired by the power scaling laws of massive MIMO [33], the transmit power at the user nodes can be scaled inversely proportional to the number of antennas at the base-station as $P_d = E_d/M$, where E_d is fixed. In this context, by letting $M \to \infty$ in (22) and by invoking (9), the SINR of the k-th user node within the asymptotic base-station antenna regime can be derived as

$$\tilde{\gamma}_k^{\infty} = \frac{\alpha \hat{\zeta}_{G_k}}{(1-\alpha)\sigma_n^2} \Psi\left(\left\| \mathbf{h}_k \mathbf{P}_E^{1/2} \right\|^2 \right) \tag{23}$$

Then, the obtained asymptotic SINR in (23) can be rewritten as $\tilde{\gamma}_k^{\infty} = \mathcal{A}_k \Psi(Z)$, where $\mathcal{A}_k = \alpha \hat{\zeta}_{G_k}/(1-\alpha)\sigma_n^2$ and $Z = \left\| \mathbf{h}_k \mathbf{P}_E^{1/2} \right\|^2 = \sum_{j=1}^{N} Z_j$ is a sum of N independent random variables that are exponentially distributed with each element having the probability density function (PDF) in the following form

$$f_{Z_j}(x) = \exp\left(\frac{-x}{\beta_{H_j} P_{E_j}} \right) / \left(\beta_{H_j} P_{E_j} \right), \quad x \geq 0. \tag{24}$$

However, when all Z_js are independent but not identically distributed (i.n.i.d.) with distinct average powers, then the PDF of Z is given by [34]

$$f_Z(z) = \sum_{j=1}^{N} \frac{\Omega_j}{\beta_{H_j} P_{E_j}} \exp\left(\frac{-z}{\beta_{H_j} P_{E_j}} \right), \quad z \geq 0. \tag{25}$$

where

$$\Omega_j = \prod_{i=1, i\neq j}^{N} \frac{\beta_{H_j} P_{E_j}}{\beta_{H_j} P_{E_j} - \beta_{H_i} P_{E_i}}. \tag{26}$$

Thus, the average sum rate can be written as

$$\bar{\mathcal{R}}_U^{\infty} = (1-\alpha) \sum_{k=1}^{K} \int_0^{\infty} \log_2 \left(1 + \mathcal{A}_k \Psi(z) \right) f_Z(z) dz. \tag{27}$$

However, the above expression is mathematically intractable due to the non-linearity of energy harvesting model, and hence, the linear model is considered here as an approximation. Accordingly, the average sum rate in (27) with the linear model for energy harvesting can be rewritten as follows:

$$\bar{\mathcal{R}}_U^{\infty} \approx (1-\alpha) \sum_{k=1}^{K} \int_0^{\infty} \log_2 \left(1 + \eta \mathcal{A}_k z \right) f_Z(z) dz. \tag{28}$$

Thereby, this integral can be solved using [35, Equation (4.337.2)], and then, the achievable sum rate can be derived in closed-form as shown in (29) at the top of the previous page, where $\mathrm{Ei}(\cdot)$ is the exponential integral function [35].

Remark 1: Both uplink sum rate expressions are monotonically increasing functions with the number of active jammers (N), and thus, massive MIMO systems can take advantage of the jamming attacks for boosting the achievable rate, while evidently maintaining the secrecy performance through other efficient secure transmission techniques.

C. Optimization of time-switching factor

In time-switching energy harvesting protocol, the energy harvesting and data transmissions are successively taking place in two orthogonal time-slots αT and $(1-\alpha)T$, respectively. Thus, finding the optimal allocated time for each phase, i.e. the optimal time-switching factor (α), has a considerable impact on the system performance. To this end, two optimization problems are formulated in this subsection to achieve α optimality based on maximizing the achievable sum rate and ensuring data rate user-fairness, respectively.

1) Sum Rate Maximization: Sum rate is an important indicator for system performance and it is of great interest to Massive MIMO systems in order to provide good service under favorable propagation [36]. Thus, the asymptotic expression of the achievable uplink sum rate in (23) can be utilized for the optimization problem of finding the optimal time switching factor (α) as detailed below

$$\begin{aligned}\alpha^* &= \underset{0\le\alpha\le 1}{\text{maximize}} \;\; \bar{\mathcal{R}}_U^{\infty} \\ &= \underset{0\le\alpha\le 1}{\text{maximize}} \;\; (1-\alpha)\sum_{k=1}^{K}\log_2(1+\tilde{\gamma}_k^{\infty}) \\ &= \underset{0\le\alpha\le 1}{\text{maximize}} \;\; (1-\alpha)\sum_{k=1}^{K}\log_2\left(1+\frac{\alpha\hat{\zeta}_{G_k}\left\|\mathbf{h}_k\mathbf{P}_E^{1/2}\right\|^2}{(1-\alpha)\sigma_n^2}\right) \end{aligned} \quad (30)$$

The partial derivative of $\bar{\mathcal{R}}_U^{\infty}$ with respective to α can be derived as

$$\frac{\partial\bar{\mathcal{R}}_U^{\infty}}{\partial\alpha} = \sum_{k=1}^{K}\frac{\nu_k}{1-\alpha(1-\nu_k)} - \sum_{k=1}^{K}\ln\left(1+\frac{\nu_k\alpha}{1-\alpha}\right), \quad (31)$$

where ν_k is given by

$$\nu_k = \frac{\hat{\zeta}_{G_k}}{\sigma_n^2}\sum_{k=1}^{K}\left\|\mathbf{h}_k\mathbf{P}_E^{1/2}\right\|^2. \quad (32)$$

By letting $\partial\bar{\mathcal{R}}_U^{\infty}/\partial\alpha = 0$, it can be shown that

$$\sum_{k=1}^{K}\frac{\nu_k}{1-\alpha(1-\nu_k)} = \sum_{k=1}^{K}\ln\left(1+\frac{\nu_k\alpha}{1-\alpha}\right), \quad (33)$$

Next, by exploiting the fact that the achievable sum rate maximizes when the achievable rates of individual user nodes are maximized, (33) can be simplified as

$$\exp\left(\frac{\nu_k}{1-\alpha(1-\nu_k)}\right) = \frac{1-\alpha(1-\nu_k)}{1-\alpha}, \quad (34)$$

The derived expression in (34) can be re-arranged as follow:

$$\left(\frac{(1-\alpha)(\nu_k-1)}{1-\alpha(1-\nu_k)}\right)\exp\left(\frac{(1-\alpha)(\nu_k-1)}{1-\alpha(1-\nu_k)}\right) = \left(\frac{\nu_k-1}{e}\right) \quad (35)$$

where $e=\exp(1)$.

Next, by using the fact that the solution for $f(x)\exp(f(x)) = y$ is $f(x) = \mathbb{W}(y)$, where $\mathbb{W}(\cdot)$ is the Lambert-W function [37], and hence, (35) can be re-written as:

$$\mathbb{W}\left(\frac{\nu_k-1}{e}\right) = \frac{(1-\alpha)(\nu_k-1)}{1-\alpha(1-\nu_k)}. \quad (36)$$

By using (36), the optimal α that maximizes the achievable uplink sum rate can be derived as follows:

$$\alpha^* = \frac{\nu_k - 1 - \mathbb{W}\left(\frac{\nu_k-1}{e}\right)}{(\nu_k-1)\left(\mathbb{W}\left(\frac{\nu_k-1}{e}\right)+1\right)}. \quad (37)$$

The second partial derivative of the achievable rate for the k-th user node with respect to α can be derived as

$$\frac{\partial^2[\bar{\mathcal{R}}_U^{\infty}]_k}{\partial\alpha^2} = \frac{-\nu_k^2}{(1-\alpha)(\alpha\nu_k-\alpha+1)^2} < 0 \quad (38)$$

By considering the fact of $\alpha\in[0,1]$, it can be concluded that $\partial^2[\bar{\mathcal{R}}_U^{\infty}]_k/\partial\alpha^2 < 0$ for all α. Therefore, the optimal α derived in (37) indeed maximizes the achievable sum rate.

2) Max-Min Optimization: The performance optimization while guaranteeing user-fairness in terms of the harvested energy and achievable uplink rate of the user nodes has a significant impact in such compelling scenario in order to fully exploit the available resources [38]. Therefore, we will show that the time-switching factor can be optimized based on the maximum fairness criterion, a max-min optimization problem is formulated by first setting the user SINR targets equal to a common SINR ($\bar{\gamma}_k$), and then searching for the maximum value of the common SINR as follows

$$\begin{aligned} \underset{\alpha\;\forall k}{\text{maximize}} \quad & \bar{\gamma}_k && (39a)\\ \text{subject to} \quad & \bar{\gamma}_k\Delta_k \ge P_{d_k}(M-K)\hat{\zeta}_{G_k}, \;\; \forall k, && (39b)\\ & 0\le\alpha\le 1, \;\; \forall k, && (39c)\end{aligned}$$

where $\Delta_k = \sum_{k'=1}^{K}P_{d_{k'}}(\zeta_{G_{k'}}-\hat{\zeta}_{G_{k'}})+\sigma_n^2$. Since the objective function in this optimization problem is a monomial and the constrains are posynomials, this is a geometric program which can be solved by using CVX tool for disciplined convex programming to find the optimal time-switching factor α^*.

Remark 2: Since users and jammers are spatially-distributed, both transmission and harvesting channels experience distinctive path-losses within a coherence block. Therefore, user fairness must be jointly guaranteed in terms of both energy and rate in order to overcome the near-far effects and obtain optimal levels of harvested energy and data rate.

D. Rate-energy trade-off

In time-switching protocol, the energy harvesting and data transfers carry out over two sequential time-slots. In details, the harvested energy is a monotonically increasing function of α, while on the contrary the achievable uplink rate is a monotonically decreasing function of α. Thereby, the rate-energy trade-off can be obtained by first solving for α in (6) and then by substituting the result into (22) as elaborated below

$$\begin{aligned}\bar{\mathcal{R}}_U^{*} \approx \sum_{k=1}^{K}&\left(\frac{T}{T_C} - \frac{\bar{E}_h}{\left(T_C\sum\limits_{n=1}^{N}\Psi_{EH_k}\left(P_{E_n}\beta_{H_{kn}}\right)\right)}\right)\\ &\times\log_2\left(1+\frac{\theta_{d_k}(M-K)\hat{\zeta}_{G_k}}{\sum\limits_{k'=1}^{K}\theta_{d_{k'}}(\zeta_{G_{k'}}-\hat{\zeta}_{G_{k'}})+\sigma_n^2}\right),\end{aligned} \quad (40)$$

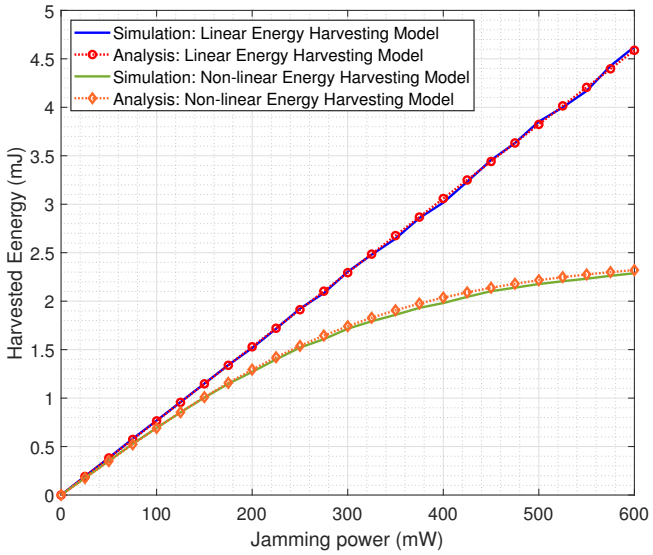

Fig. 3. A comparison between the linear and non-linear energy harvesting models with respect to the jamming power.

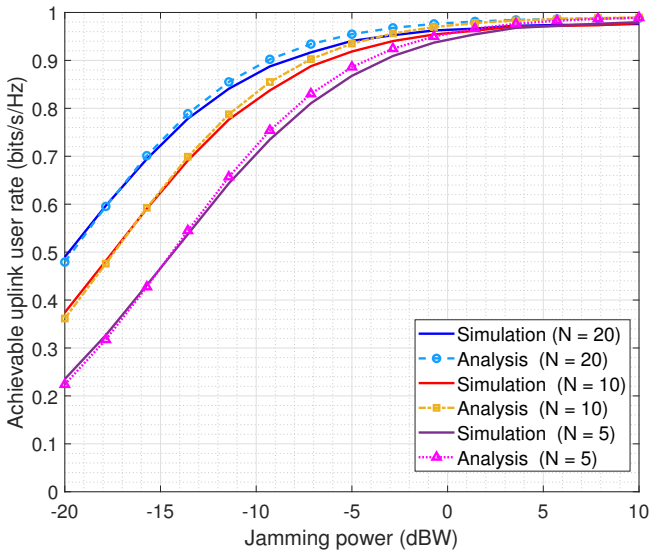

Fig. 4. Achievable uplink user rate versus jamming power when $K = 5$, $M = 20$, $\alpha = 0.5$, and different number of active attackers (N).

where θ_{d_k} is defined as

$$\theta_{d_k} = \frac{\bar{E}_h \sum_{n=1}^{N} \Psi_{EH_k}\left(P_{E_n}\beta_{H_{kn}}\right)}{T \sum_{n=1}^{N} \Psi_{EH_k}\left(P_{E_n}\beta_{H_{kn}}\right) - \bar{E}_h}. \tag{41}$$

Remark 3: The energy-rate trade-off expression in (40) is optimal due to the max-min user-fairness when setting the harvested energy targets of each user to a common value $\bar{E}_h$. Thereby, the max-min optimal time-switching factor corresponding to any system operating point can be attained by applying this optimal energy-rate trade-off.

IV. Numerical Results

In this section, we evaluate the performance of the proposed energy harvesting scheme. To capture the effects of practical transmission impairments, the channel pathloss is modeled as $[\mathrm{PL}]_{\mathrm{dB}} = \mathrm{PL}_0 + 10v\log d/d_0$, where d, d_0, PL_0 and v are defined as the distance between the transmitter and receiver, a reference distance, the pathloss at the reference distance, and the pathloss exponent, respectively. Unless otherwise specified, the simulation parameters are set to $v = 2.3$, $d_0 = 100\,\mathrm{m}$, $d_G = 100 - 300$ m, $d_H = 100 - 500$ m, $\sigma_n^2 = 0\,\mathrm{dBW}$, and $\mathcal{P}_P = 0\,\mathrm{dBW}$. The coherence time is set to $T_C = 1\mathrm{ms}$ having 196 symbols, pilot length is $T_p = K$ [29].

First, we will evaluate the discrepancy between the properties of the non-linear energy harvesting model and the linear model that is typically assumed in the energy harvesting research. To this end, Fig. 3 presents a comparison between the harvested energy of the nonlinear and conventional linear in [1] for time-switching protocol in the studied system. The simulation curves for the linear model are plotted using Monte-Carlo simulations by keeping the RF-to-DC conversion efficiency (η) fixed at 0.65. The analytical curves for the non-linear model are plotted by using (6). Clearly, the obtained results from this Fig. 3 verify that the linear energy harvesting model miscalculates the harvested energy by neglecting the non-linearity of practical energy harvesting rectenna circuits.

In Fig. 4, the average achievable user data rate at the base-station in the finite antenna regime is plotted against the jamming power by considering different numbers of active jammers (N). The analytical uplink rate curves are plotted by using (22), and are compared to the Monte-Carlo simulations of the uplink rate expression in (14). Obviously, the achievable rate gradually increases when the jammers transmit higher power levels because the more jamming power, the greater energy will be harvested by the user nodes until a saturation point. This is an explicit consequence of the saturation effect of the non-linear energy harvesting model. Moreover, increasing the number of jamming attacks in the proximity of the served area contributes to harvest more energy and eventually achieves higher data rate. Our analysis is compared to the Monte Carlo simulations to validate that the derived achievable rate by using the worst-case Gaussian technique provides a tight lower bound to the achievable rate.

The asymptotic uplink sum rate is plotted as a function of the time switching factor (α) in Fig. 5 for the infinite antenna regime at the base-station, i.e. with progressively increasing the number of antennas M. The asymptotic sum rate curves are plotted by using (29) and compared to the Monte-Carlo simulations in order for validating the accuracy of our analysis. Fig. 5 reveals that the theoretical/asymptotic sum rate limits in (29) can be attained when the number of base-station antennas grows large. Additionally, we notice the following essential design insights. The sum rate approaches its maximum at the optimal α and then decreases thereafter. When α is small, the harvested energy by the user nodes is not adequate to achieve high sum rate. Nonetheless, a too large α value leads to more harvested energy but less residual time for the data transmission, which degrades the sum data rate performance. Thus, there exists a fundamental trade-off between harvested

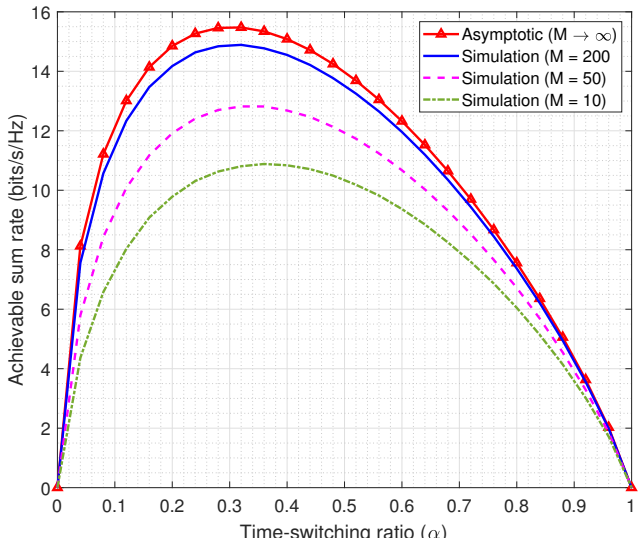

Fig. 5. Achievable uplink sum rate versus time-switching factor (α) for different number of base-station antennas (M) when $K = 5$ and $N = 5$.

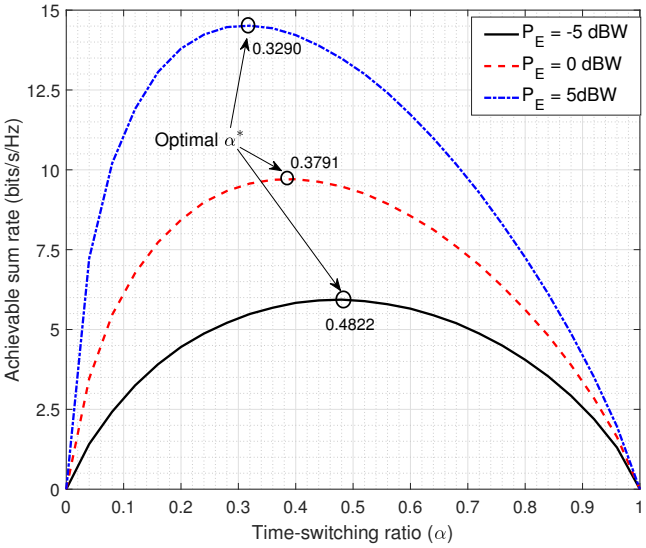

Fig. 6. Optimization of time-switching factor (α) for maximizing the achievable uplink sum rate with considering different levels of jamming power.

energy and uplink data rate, which will be further explored in the forthcoming evaluation results.

The proposed optimization problem for maximizing the uplink sum rate with respect to the time-switching factor (α) is investigated in Fig. 6 for different values of the jamming powers. Specifically, the achievable sum rate is plotted against α where the optimal α^* is calculated by closed-form solution of (37). Fig. 6 shows that the sum rate versus α is a convex function. Clearly, the achievable rate increases with α when $\alpha \leq \alpha^*$, and then decreases if $\alpha > \alpha^*$. Accordingly, the maximum achievable rate is attained at α^*, which is consistent with the obtained analytical results for maximizing the sum rate in Section III-C1. Further, the optimal α^* itself deceases when there is more jamming power to harvest, which eventually spares more time for data transmission and increases the sum data rate. This observation verifies that the proposed jamming energy harvesting scheme is beneficial in boosting the performance of massive MIMO systems.

The proposed max-min fairness-based problem for optimizing α to achieve a common data rate among the served users is evaluated in Fig. 7. For the comparison purposes, the achievable user rates is plotted against the harvested energy, when α increases from 0.2 to 1, for (i) the equal power allocation scheme and (ii) optimal power allocation with max-min fairness policy. The considered users are spatially distributed as $\mathbf{d_G} = [150,\ 180,\ 220,\ 250]$ m. The power allocation coefficients for the optimal power allocation are computed by solving the geometric program in (39a)-(39c) using MATLAB CVX. The individual user data rate with the equal power control is mainly affected by the channel conditions or the spatial location of the distributed users. For instance, when the equal power allocation policy is employed, the nearest user (User 1) obtains the best data rate trade, while the farthest user (User 4) experiences the lowest data rate. Clearly, the equal power allocation policy does not guarantee fairness in terms of user data rate. Nevertheless, the proposed max-min fairness

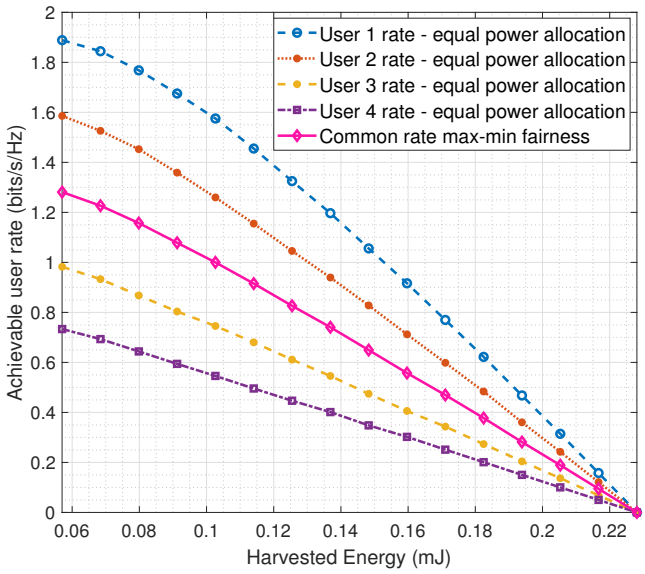

Fig. 7. A comparison of the achievable uplink data rate and the harvested energy between the uniform and max-min user-fairness power allocation policies.

power control provides a common achievable rate for every user regardless of its spatial location. Thereby, the proposed max-min power allocation jointly guarantees user-fairness in terms of both the achievable rate and harvested energy. Thus, the validity of the analytical results is corroborated.

The analysis of the rate-energy trade-off in Section III-D is investigated in Fig. 8. Specifically, the achievable uplink sum rate with respect to the harvested energy at the user nodes is plotted for different number of jammers (N) in the finite base-station antenna regime. We used the derived rate-energy trade-off expression in (40) to plot the analytical curves. Fig. 8 clearly reveals that the uplink achievable rate becomes a maximum when the harvested energy approaches the common

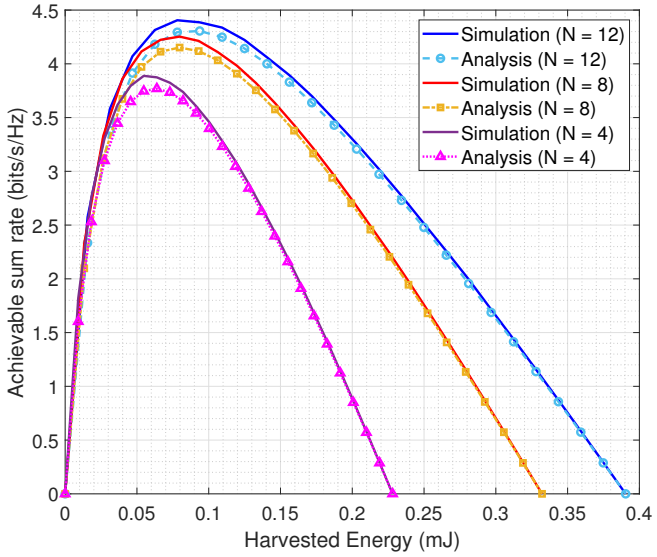

Fig. 8. The rate-energy trade-off. A comparison between uplink sum rate versus the harvested energy for $K = 4$, $M = 15$.

rate-energy trade-offs. However, the achievable uplink data rate becomes infinitesimal when α approaches one, whereas the harvested energy becomes a maximum value due to the fact that the users harvest energy for the entire transmission frame. Further, as mentioned earlier the harvested energy increases with N, which leads to increased achievable sum rates due to the higher transmission powers of the user nodes. This observation validates the insights summarized in Remark 1, and Monte-Carlo simulations validate our analysis in (40).

V. Conclusion

In this paper, we proposed an energy harvesting scheme that exploits the jamming transmissions of the active attackers in multi-user massive MIMO systems. Specifically, a wireless-powered multi-user massive MIMO system has been considered where user nodes harvest energy from the jammers and utilize it for information transmission. The feasibility of proposed concept has been investigated by system performance analysis for a training-based massive MIMO involves imperfectly estimated CSI at the base-station and employing the time-switching protocol. In particular, the harvested energy, SINR, and sum rate expressions have been derived for finitely many base-station antennas, where a tight sum rate expression is obtained in closed-form. The asymptotic performance metrics are also provided when the numbers of base-station antennas grow large. In addition, two optimization problems are provided and solved to achieve optimal time switching factor based on maximizing the uplink sum rate and jointly ensuring user-fairness in terms of energy and rate. Furthermore, the fundamental trade-off between the harvested energy and achievable sum rate are quantified in closed-form expression. Finally, the performance metrics have been analytically and numerically evaluated over various antenna configurations and setups where the obtained results have validated the feasibility of the proposed energy harvesting scheme in boosting the massive MIMO uplink performance.

References

[1] H.Al-Hraishawi, S. Chatzinotas, and B. Ottersten, "Exploiting jamming attacks for energy harvesting in massive MIMO systems," in *IEEE Int. Conf on Commun. (ICC)*, Jun. 2021, pp. 1–6.

[2] F. Tariq, M. R. A. Khandaker, K. Wong, M. A. Imran, M. Bennis, and M. Debbah, "A speculative study on 6G," *IEEE Wireless Commun.*, vol. 27, no. 4, pp. 118–125, 2020.

[3] M. Wang, Y. Lin, Q. Tian, and G. Si, "Transfer learning promotes 6G wireless communications: Recent advances and future challenges," *IEEE Trans. Reliability*, vol. 70, no. 2, pp. 790–807, 2021.

[4] Z. Ding, C. Zhong, D. Wing Kwan Ng, M. Peng, H. A. Suraweera, R. Schober, and H. V. Poor, "Application of smart antenna technologies in simultaneous wireless information and power transfer," *IEEE Commun. Mag.*, vol. 53, no. 4, pp. 86–93, 2015.

[5] H. Al-Hraishawi and G. A. A. Baduge, "Wireless energy harvesting in cognitive massive MIMO systems with underlay spectrum sharing," *IEEE Wireless Commun. Lett.*, vol. 6, no. 1, pp. 134–137, Feb. 2017.

[6] L. Chen, F. R. Yu, H. Ji, B. Rong, X. Li, and V. C. M. Leung, "Green full-duplex self-backhaul and energy harvesting small cell networks with massive MIMO," *IEEE J. Sel. Areas Commun.*, vol. 34, no. 12, pp. 3709–3724, Dec. 2016.

[7] H. Wang, W. Wang, X. Chen, and Z. Zhang, "Wireless information and energy transfer in interference aware massive MIMO systems," in *IEEE Globel Comnun. Conf. (Globecom)*, Dec. 2014, pp. 2556–2561.

[8] D. Kudathanthirige, R. Shrestha, and G. A. A. Baduge, "Wireless information and power transfer in relay-assisted downlink massive MIMO," *IEEE Trans. Green Commun. Netw.*, vol. 3, no. 3, pp. 789–805, 2019.

[9] M. Alageli, A. Ikhlef, and J. Chambers, "Swipt massive MIMO systems with active eavesdropping," *IEEE J. Sel. Areas Commun.*, vol. 37, no. 1, pp. 233–247, 2019.

[10] L. Liu and W. Yu, "Massive connectivity with massive MIMO–Part I: Device activity detection and channel estimation," *IEEE Trans. Signal Process.*, vol. 66, no. 11, pp. 2933–2946, 2018.

[11] H. Al-Hraishawi and G. Amarasuriya, "Sum rate analysis of cognitive massive MIMO systems with underlay spectrum sharing," in *IEEE Globel Comnun. Conf. (Globecom)*, Apr. 2016, pp. 1–7.

[12] M. Vanhoef and F. Piessens, "Advanced Wi-Fi attacks using commodity hardware," in *Proc. 30th Annu. Comput. Secur. Appl. Conf. (ACSAC)*, New Orleans, LA, USA, Dec. 2014, pp. 256–265.

[13] X. Zhou, B. Maham, and A. Hjorungnes, "Pilot contamination for active eavesdropping," *IEEE Trans. Wireless Commun.*, vol. 11, no. 3, pp. 903–907, Mar. 2012.

[14] D. Kapetanovic, G. Zheng, and F. Rusek, "Physical layer security for massive MIMO: An overview on passive eavesdropping and active attacks," *IEEE Commun. Mag.*, vol. 53, no. 6, pp. 21–27, Jun. 2015.

[15] Y. O. Basciftci, C. E. Koksal, and A. Ashikhmin, "Securing massive MIMO at the physical layer," in *IEEE Conf. on Commun. and Netw. Secur. (CNS)*, Philadelphia, PA, USA, 2015.

[16] T. T. Nguyen and K.-K. Nguyen, "Anti-jamming in cell free mMIMO systems," in *IEEE Globel Comnun. Conf. (Globecom)*, 2021, pp. 1–6.

[17] Z. Shen, K. Xu, and X. Xia, "Beam-domain anti-jamming transmission for downlink massive MIMO systems: A stackelberg game perspective," *IEEE Trans. Inf. Forensics Security*, vol. 16, pp. 2727–2742, 2021.

[18] T. T. Do, E. Bjornson, E. G. Larsson, and S. M. Razavizadeh, "Jamming-resistant receivers for the massive MIMO uplink," *IEEE Trans. Inf. Forensics Security*, vol. 13, no. 1, pp. 210–223, Jan. 2018.

[19] W. Xu, B. Li, L. Tao, and W. Xiang, "Artificial noise assisted secure transmission for uplink of massive MIMO systems," *IEEE Trans. Veh. Technol.*, vol. 70, no. 7, pp. 6750–6762, 2021.

[20] H. Al-Hraishawi, G. Baduge, and R. Schaefer, "Artificial noise-aided physical layer security in underlay cognitive massive MIMO systems with pilot contamination," *Entropy*, vol. 19, no. 7, p. 349, Jul 2017.

[21] D. Kudathanthirige and G. A. A. Baduge, "Effects of pilot contamination attacks in multi-cell multi-user massive MIMO relay networks," *IEEE Trans. Commun.*, vol. 67, no. 6, pp. 3905–3922, 2019.

[22] H. Al-Hraishawi, G. Amarasuriya, and R. F. Schaefer, "Secure communication in underlay cognitive massive mimo systems with pilot contamination," in *GLOBECOM 2017 - 2017 IEEE Global Communications Conference*, Singapore, Dec. 2017, pp. 1–7.

[23] N. Akbar, S. Yan, A. M. Khattak, and N. Yang, "On the pilot contamination attack in multi-cell multiuser massive MIMO networks," *IEEE Trans. Commun.*, vol. 68, no. 4, pp. 2264–2276, 2020.

[24] J. Xu, W. Xu, D. W. K. Ng, and A. L. Swindlehurst, "Secure communication for spatially sparse millimeter-wave massive MIMO channels via hybrid precoding," *IEEE Trans. Commun.*, vol. 68, no. 2, pp. 887–901, 2020.

[25] Z. Fang, T. Song, and T. Li, "Energy harvesting for two-way ofdm communications under hostile jamming," *IEEE Signal Processing Letters*, vol. 22, no. 4, pp. 413–416, 2015.

[26] E. V. Belmega and A. Chorti, "Protecting secret key generation systems against jamming: Energy harvesting and channel hopping approaches," *IEEE Trans. Inf. Forensics Security*, vol. 12, no. 11, pp. 2611–2626, 2017.

[27] G. Rezgui, E. V. Belmega, and A. Chorti, "Mitigating jamming attacks using energy harvesting," *IEEE Wireless Commun. Lett.*, vol. 8, no. 1, pp. 297–300, 2019.

[28] T. L. Marzetta, "Noncooperative cellular wireless with unlimited numbers of base station antennas," *IEEE Trans. Wireless Commun.*, vol. 9, no. 11, pp. 3590–3600, Nov. 2010.

[29] T. L. Marzetta, E. G. Larsson, H. Yang, and H. Q. Ngo, *Fundamentals of Massive MIMO*. Cambridge University Press, 2016.

[30] S. M. Kay, *Fundamentals of Statistical Signal Processing: Practical: Algorithm Development*. Upper Saddle River, NJ, USA: Prentice-Hall, Inc., 1993.

[31] E. Boshkovska, D. W. K. Ng, N. Zlatanov, and R. Schober, "Practical non-linear energy harvesting model and resource allocation for swipt systems," *IEEE Commun. Lett.*, vol. 19, no. 12, pp. 2082–2085, 2015.

[32] A. M. Tulino and S. Verdu, "Random matrix theory and wireless communications," *Foundations Trends Commun. Inf. Theory*, vol. 1, no. 1, pp. 1–128, Jun. 2004.

[33] H. Q. Ngo, E. G. Larsson, and T. L. Marzetta, "Energy and spectral efficiency of very large multiuser MIMO systems," *IEEE Trans. Commun.*, vol. 61, no. 4, pp. 1436–1449, Apr. 2013.

[34] J. Proakis, *Digital communications*, 4th ed. New York:McGraw-Hill, Inc., 2001.

[35] I. Gradshteyn and I. Ryzhik, *Table of integrals, Series, and Products*, 7th ed. Academic Press, 2007.

[36] H. Yang and T. L. Marzetta, "Massive MIMO with max-min power control in line-of-sight propagation environment," *IEEE Trans. Commun.*, vol. 65, no. 11, pp. 4685–4693, 2017.

[37] R. M. Corless, G. H. Gonne, D. E. G. Hare, D. J. Jeffrey, and D. E. Knuth, "On the Lambert W function," *Adv. Comput. Math.*, vol. 5, no. 1, pp. 329–359, 1996.

[38] H. Al-Hraishawi, G. A. Aruma Baduge, H. Q. Ngo, and E. G. Larsson, "Multi-cell massive MIMO uplink with underlay spectrum sharing," *IEEE Trans. on Cogn. Commun. Netw.*, vol. 5, no. 1, pp. 119–137, 2019.